

# Excited states of the hydrogen molecule in magnetic fields: The singlet $\Sigma$ states of the parallel configuration

P. Schmelcher, T. Detmer and L. S. Cederbaum  
*Theoretische Chemie, Physikalisch-Chemisches Institut,  
Universität Heidelberg, INF 229, D-69120 Heidelberg,  
Federal Republic of Germany*

Excited states of the hydrogen molecule subject to a homogeneous magnetic field are investigated for the parallel configuration in the complete regime of field strengths  $B = 0 - 100a.u.$ . Up to seven excitations are studied for gerade as well as ungerade spin singlet states of  $\Sigma$  symmetry with a high accuracy. The evolution of the potential energy curves for the individual states with increasing field strength as well as the overall behaviour of the spectrum are discussed in detail. A variety of phenomena like for example the sequence of changes for the dissociation channels of excited states and the resulting formation of outer wells are encountered. Possible applications of the obtained data to the analysis of magnetic white dwarfs are outlined.

## I. INTRODUCTION

Matter which is exposed to strong external magnetic fields changes its basic properties and structure and leads to a variety of new phenomena. As a result strong fields are of importance in different branches of physics like atomic, molecular or solid state physics. For atomic and molecular systems there are two prominent possibilities to encounter the strong field regime: highly excited Rydberg states in the laboratory and atoms and molecules in the atmospheres of magnetized white dwarfs (see refs. [1–3] for a compilation of the subject). From a theorists point of view particle systems in strong fields pose a hard problem due to several competing interactions (Coulomb attraction and repulsion, para- and diamagnetic interactions). Of particular interest, but most complicated to investigate, is hereby the so-called intermediate regime which is characterized by comparable magnetic and Coulomb binding forces. Focusing on the low-lying states of atoms and molecules we envisage this regime for those magnetic white dwarfs which possess field strengths in the regime  $10^3 - 10^5 T$ . Each magnetic white dwarf possesses a characteristic regime of field strengths which varies, in case of a dipole, by a factor of two from the pole to the equator. To perform a first identification of observed spectra from the atmospheres of these objects one uses the so-called stationary line spectroscopy: characteristic absorption features can appear only for those wavelengths which correspond to an extremum of the transition wavelength with respect to the field strength. In a second step one then performs simulations of the radiation transport in the atmosphere in order to obtain synthetic spectra. In the eighties the above approaches have been used to identify hydrogen in a number of magnetized white dwarfs [4–7]. Recently the stationary line argument has been successfully [8] used to obtain strong evidence for helium in the spectrum of the magnetic white dwarf GD229 whose absorption features have been mysterious ever since its discovery 25 years ago. This was only possible due to the enormous progress achieved with respect to our knowledge of the spectrum and transitions of the helium atom in strong magnetic fields [9, 10]. However, this should not obscure the fact that there are a number of magnetic white dwarfs whose spectra remain unexplained and furthermore new magnetic objects are discovered (see, for example, Reimers et al [11] in the course of the Hamburg survey of the European Southern Observatory (ESO)). Very recently strong candidates for quasimolecular absorption features have been discovered in magnetized white dwarfs [12]. This raises the demand for a theoretical investigation of molecular properties, in particular of the hydrogen molecule, in such strong fields.

Several theoretical investigations were performed for molecular systems in strong magnetic fields. Most of them deal with the electronic structure of the  $H_2^+$  ion (see refs. [13–19] and references therein). Very interesting phenomena can be observed already for this simple diatomic system. For the ground state of the  $H_2^+$  molecule the dissociation energy increases and the equilibrium internuclear distance simultaneously decreases with increasing field strength. Furthermore it was shown [18, 19] that a certain class of excited electronic states, which possess a purely repulsive potential energy surface in the absence of a magnetic field, acquire a well-pronounced potential well in a sufficiently strong magnetic field. Moreover the electronic potential energies depend not only on the internuclear distance but also on the angle between the magnetic field and the molecular axis which leads to a very complex topological behavior of the corresponding potential energy surfaces [14–16].

In contrast to the  $H_2^+$  ion there exist only a few investigations dealing with the electronic structure of the hydrogen

molecule in the presence of a strong magnetic field. Highly excited states of  $H_2$  were studied for a field strength of 4.7  $T$  in ref. [20]. For intermediate field strengths two studies of almost qualitative character investigate the potential energy curve (PEC) of the lowest  $^1\Sigma_g$  state [21, 22]. A few investigations were performed in the high field limit [23–26], where the magnetic forces dominate over the Coulomb forces and therefore several approximations can be used. Very recently a first step has been done in order to elucidate the electronic structure of the  $H_2$  molecule for the parallel configuration, i.e. for parallel internuclear and magnetic field axes [27–30]. Hereby refs. [27, 28] apply an exact, i.e. fully correlated approach, whereas refs. [29, 30] use Hartree-Fock calculations and focus exclusively on the identification of the global ground state of the molecule. In refs. [27, 28] the lowest states of the  $\Sigma$  and  $\Pi$  manifolds were studied for gerade and ungerade parity as well as singlet and triplet spin symmetry. Hereby accurate adiabatic electronic energies were obtained for a broad range of field strengths from field free space up to strong magnetic fields of 100  $a.u.$  A variety of interesting effects were revealed. As in the case of the  $H_2^+$  ion, the lowest strongly bound states of  $\Sigma$  symmetry, i.e. the lowest  $^1\Sigma_g$ ,  $^3\Sigma_g$  and  $^1\Sigma_u$  state, show a decrease of the bond length and an increase of the dissociation energy for sufficiently strong fields. Furthermore a change in the dissociation channel occurs for the lowest  $^1\Sigma_u$  state between  $B = 10.0$  and  $20.0 a.u.$  due to the existence of strongly bound  $H^-$  states in the presence of a magnetic field. The  $^3\Sigma_g$  state was shown to exhibit an additional outer minimum for intermediate field strengths which could provide vibrationally bound states.

An important result of refs. [27, 29] is the change of the ground state from the lowest  $^1\Sigma_g$  state to the lowest  $^3\Sigma_u$  state between  $B = 0.1$  and  $0.2 a.u.$  This crossing is of particular relevance for the binding properties of the global ground state of the molecule: The  $^3\Sigma_u$  state is an unbound state and possesses only a very shallow van der Waals minimum which does not support any vibrational level. Therefore, the global ground state of the hydrogen molecule for the parallel configuration is an unbound state for  $B \gtrsim 0.2 a.u.$ . Furthermore it has been shown in ref. [25] that for very strong fields ( $B \gtrsim 3 \times 10^3 a.u.$ ) the strongly bound  $^3\Pi_u$  state is the global ground state of the hydrogen molecule oriented parallel to the magnetic field. Finally the complete scenario for the crossovers of the global ground state of the parallel configuration has been clarified in ref. [28] which contains the transition field strengths for the crossings among the lowest states of  $^1\Sigma_g$ ,  $^3\Sigma_u$  and  $^3\Pi_u$  symmetry.

The above considerations show that detailed studies of the electronic properties of the hydrogen molecule in a magnetic field are very desirable. The present investigation deals with the excited  $\Sigma$  states of the hydrogen molecule in the parallel configuration which is distinct by its higher symmetry [31]. We employ a full configuration interaction (CI) approach which is most suitable for obtaining detailed information on the electronic structure. Our investigation is divided into two separate studies: the first and present work focuses on singlet states of both gerade and ungerade symmetry whereas a later investigation will focus on the corresponding triplet states again for both parities. Due to the spin Zeeman splitting the spin singlet and triplet manifolds are increasingly separated with increasing field strength. The spin character provides therefore a natural dividing line of our extensive work which contains a large amount of information and data on the behaviour of the excited states of the molecule. The results of our calculations include accurate adiabatic PECs for the complete range of field strengths  $0 \leq B \leq 100 a.u.$ . Up to seven excited states have been investigated for each symmetry. We present detailed data for the total and dissociation energies at the equilibrium internuclear distances as well as the equilibrium positions themselves for the lowest three excitations for each symmetry. Due to the large amount of data the evolution of the higher excited states with increasing field strength is presented only graphically. However, further informations like, for example, the positions of the maxima and the accurate heights of the barriers or the complete data of the PEC's as well as numerical data on the higher excited states, more precisely, on the fourth up to the seventh excited state, can be obtained from the authors upon request.

In detail the paper is organized as follows. In section II we describe the theoretical aspects of the present investigation, including a discussion of the Hamiltonian, a description of the atomic orbital basis set and some remarks on the CI approach. Section III contains the results and an elaborate discussion of the evolution of the electronic structure in the presence of the magnetic field with increasing strength.

## II. THEORETICAL ASPECTS

Our starting point is the total nonrelativistic molecular Hamiltonian in Cartesian coordinates. The total pseudomomentum is a constant of motion and therefore commutes with the Hamiltonian [32, 33]. For that reason the Hamiltonian can be simplified by performing a so-called pseudoseparation of the center of mass motion [32, 34, 35] which introduces the center of mass coordinate and the conserved pseudomomentum as a pair of canonical conjugated variables. Further simplifications can be achieved by a consecutive series of unitary transformations [34, 35].

In order to separate the electronic and nuclear motion we perform the Born-Oppenheimer approximation in the presence of a magnetic field [34–36]. As a first order approximation we assume infinitely heavy masses for the nuclei.

The origin of our coordinate system coincides with the midpoint of the internuclear axis of the hydrogen molecule and the protons are located on the  $z$  axis. The magnetic field is chosen parallel to the  $z$  axis of our coordinate system and the symmetric gauge is adopted for the vector potential. The gyromagnetic factor of the electron is chosen to be equal to two. The Hamiltonian, therefore, takes on the following appearance:

$$H = \sum_{i=1}^2 \left\{ \frac{1}{2} \mathbf{p}_i^2 + \frac{1}{8} (\mathbf{B} \times \mathbf{r}_i)^2 + \frac{1}{2} \mathbf{L}_i \mathbf{B} - \frac{1}{|\mathbf{r}_i - \mathbf{R}/2|} - \frac{1}{|\mathbf{r}_i + \mathbf{R}/2|} \right\} + \frac{1}{|\mathbf{r}_1 - \mathbf{r}_2|} + \frac{1}{R} + \mathbf{S} \mathbf{B} \quad (1)$$

The symbols  $\mathbf{r}_i$ ,  $\mathbf{p}_i$  and  $\mathbf{L}_i$  denote the position vectors, their canonical conjugated momenta and the angular momenta of the two electrons, respectively.  $\mathbf{B}$  and  $\mathbf{R}$  are the vectors of the magnetic field and internuclear distance, respectively and  $R$  denotes the magnitude of  $\mathbf{R}$ . With  $\mathbf{S}$  we denote the vector of the total electronic spin. Throughout the paper we will use atomic units.

The Hamiltonian (1) commutes with the following independent operators: the parity operator  $P$ , the projection  $L_z$  of the electronic angular momentum on the internuclear axis, the square  $S^2$  of the total electronic spin and the projection  $S_z$  of the total electronic spin on the internuclear axis. In field free space we encounter an additional independent symmetry namely the reflections of the electronic coordinates at the  $xz$  ( $\sigma_v$ ) plane. The eigenfunctions possess the corresponding eigenvalues  $\pm 1$ . This symmetry does not hold in the presence of a magnetic field! Therefore, the resulting symmetry groups for the hydrogen molecule are  $D_{\infty h}$  in field free space and  $C_{\infty h}$  in the presence of a magnetic field [31].

In order to solve the fixed-nuclei electronic Schrödinger equation belonging to the Hamiltonian (1) we expand the electronic eigenfunctions in terms of molecular configurations. In a first step the total electronic eigenfunction  $\Psi_{tot}$  of the Hamiltonian (1) is written as a product of its spatial part  $\Psi$  and its spin part  $\chi$ , i.e. we have  $\Psi_{tot} = \Psi \chi$ . For the spatial part  $\Psi$  of the wave function we use the LCAO-MO-ansatz, i.e. we decompose  $\Psi$  with respect to molecular orbital configurations  $\psi$  of  $H_2$ , which respect the corresponding symmetries (see above) and the Pauli principle:

$$\begin{aligned} \Psi &= \sum_{i,j} c_{ij} [\psi_{ij}(\mathbf{r}_1, \mathbf{r}_2) \pm \psi_{ij}(\mathbf{r}_2, \mathbf{r}_1)] \\ &= \sum_{i,j} c_{ij} [\Phi_i(\mathbf{r}_1) \Phi_j(\mathbf{r}_2) \pm \Phi_i(\mathbf{r}_2) \Phi_j(\mathbf{r}_1)] \end{aligned}$$

The molecular orbital configurations  $\psi_{ij}$  of  $H_2$  are products of the corresponding one-electron  $H_2^+$  molecular orbitals  $\Phi_i$  and  $\Phi_j$ . The  $H_2^+$  molecular orbitals are built from atomic orbitals centered at each nucleus. A key ingredient of this procedure is a basis set of nonorthogonal optimized nonspherical Gaussian atomic orbitals which has been established previously [37,38]. For the case of a  $H_2$ -molecule parallel to the magnetic field these basis functions read as follows:

$$\phi_{kl}^m(\rho, z, \alpha, \beta, \pm R/2) = \rho^{|m|+2k} (z \mp R/2)^l \exp \left\{ -\alpha \rho^2 - \beta (z \mp R/2)^2 \right\} \exp \{ im\phi \} \quad (2)$$

The symbols  $\rho = +\sqrt{x^2 + y^2}$  and  $z$  denote the electronic coordinates.  $m$ ,  $k$  and  $l$  are parameters depending on the subspace of the H-atom for which the basis functions have been optimized and  $\alpha$  and  $\beta$  are variational parameters. We remark that the nonlinear optimization of the variational parameters  $\alpha$  and  $\beta$  has to be accomplished for typically of the order of 100 atomic orbitals and is done by reproducing many excited states of the hydrogen atom for each field strength separately. It represents therefore a tedious and time consuming work which has, however, to be done with great care in order to obtain precise results for the following molecular structure calculations. For a more detailed description of the construction of the molecular electronic wave function we refer the reader to Ref. [27].

In order to determine the molecular electronic wave function of  $H_2$  we use the variational principle which means that we minimize the variational integral  $\frac{\int \Psi^* H \Psi}{\int \Psi^* \Psi}$  by varying the coefficients  $c_i$ . The resulting generalized eigenvalue problem reads as follows:

$$(\underline{H} - \epsilon \underline{S}) \mathbf{c} = \mathbf{0} \quad (3)$$

where the Hamiltonian matrix  $\underline{H}$  is real and symmetric and the overlap matrix is real, symmetric and positive definite. The vector  $\mathbf{c}$  contains the expansion coefficients. The matrix elements of the Hamiltonian matrix and the overlap matrix are certain combinations of matrix elements with respect to the optimized nonspherical Gaussian atomic orbitals. A description of the techniques necessary for the evaluation of these matrix elements is given in Ref. [27]. We mention here only that the electron-electron integrals needed a combination of numerical and analytical

techniques in order to make its rapid evaluation possible. The latter represents the CPU time dominating factor for the construction of the Hamiltonian matrix.

For the numerical solution of the eigenvalue problem (3) we used the standard NAG library. The typical dimension of the Hamiltonian matrix for each subspace varies between approximately 2000 and 5000 depending on the magnetic field strength. Depending on the dimension of the Hamiltonian matrix, it takes between 70 and 250 minutes for simultaneously calculating one point of a PEC of each subspace on a IBM RS6000 computer. The overall accuracy of our results with respect to the total energy is estimated to be typically of the order of magnitude of  $10^{-4}$  and for some cases of the order of magnitude of  $10^{-3}$ . It should be noted that this estimate is rather conservative; in some ranges of the magnetic field strength and internuclear distance, e.g., close to the separated atom limit, the accuracy is  $10^{-5}$  or even better. The positions, i.e. internuclear distances, of the maxima and the minima in the PECs were determined with an accuracy of  $10^{-2}a.u.$  Herefore about 350 points were calculated on an average for each PEC. It was not necessary to further improve this accuracy since a change in the internuclear distance about  $1 \times 10^{-2} a.u.$  results in a change in the energy which is typically of the order of magnitude of  $10^{-4}$  or smaller. The total CPU time needed to complete the present work amounts to several years on the above powerful computer.

### III. RESULTS AND DISCUSSION

To understand the influence of the external magnetic field on the electronic structure of the hydrogen molecule we first have to remind ourselves of the properties in the absence of the field. Accurate data for hydrogen are of great importance both in astrophysics as well as laboratory physics. It is a paradigm for many molecular phenomena like charge transfer, excitation, ionization or scattering processes. Indeed our CI calculations on the basis of an anisotropic Gaussian basis set provided also significant progress with respect to the knowledge of the field-free excitations of the molecule: several highly excited states have been calculated for the first time and some of the PECs for the lower lying states have been improved. The corresponding results have been presented to some detail in ref. [39] and contain elaborate information on the first eight excited singlet and triplet states for both gerade and ungerade parity. In the following we will first summarize the main properties of the excited singlet states in the absence of the field and then investigate the electronic structure in the presence of the magnetic field with increasing field strength. We hereby first deal with the gerade and subsequently with the ungerade states.

#### A. Excited gerade singlet states

##### 1. Field-free states

The investigation of the electronic states and PECs has been done for all internuclear distances considered ( $0.8 \leq R \leq 1000a.u.$ ) with the same atomic orbital basis set. The latter has been optimized to yield precise energies (accuracy  $10^{-6} - 10^{-9}$ ) of the hydrogen atom for the six lowest states for both parities for vanishing atomic magnetic quantum number. Additionally, in order to describe correlation effects, we have included basis functions with atomic magnetic quantum numbers  $1 \leq m_a \leq 5$ . The approximate number of two-particle configurations resulting from the above basis set is 3800. The accuracy of the electronic energies for the higher excited states  $n^1\Sigma_g^+$ ,  $n = 7 - 9$  ( $n$  indicates the degree of excitation) is, due to the above choice of the optimized basis set, lower than that for less excited states. Figure 1 shows the PECs for the states  $n^1\Sigma_g^+$ ,  $n = 2 - 9$  where the dotted lines represent the curves for the higher excited states  $n = 7 - 9$ . There is a large energetical gap ( $0.3 - 0.4a.u.$ ) between the ground and the excited states of  $^1\Sigma_g^+$  symmetry. The first five excited states are well-known from the literature [40]. Our calculations [39] show in most cases an agreement within  $10^{-6} - 5 \cdot 10^{-5}$  compared to the literature and in several cases also a variationally lower energy. As already mentioned the results on the higher excited states ( $n = 7 - 9$ ) have for the first time been reported very recently in ref. [39].

As can be seen from figure 1 all the PECs of the states  $n^1\Sigma_g^+$ ,  $n = 2 - 9$  possess a deep potential well around a minimum located approximately at  $R = 2a.u.$ . A particular feature occurring for most of the considered  $^1\Sigma_{g(u)}$  states is the existence of a second outer minimum and therefore the corresponding PECs exhibit a double well. Vibrational states in these outer wells [40] attracted recently significant experimental interest [41] since they allow the experimental observation of long-lived and highly excited valence states of the hydrogen molecule. The two minima of the  $3^1\Sigma_g^+$  state arise due to the fact that two different configurations of the same symmetry, namely the  $1\sigma_g 3d\sigma_g$  and the  $1\sigma_g 2s\sigma_g$  configurations, are energetically minimized at two significantly different internuclear distances. The deep outer wells of the  $n^1\Sigma_g^+$ ,  $n = 2, 4, 7$  states arise due to a series of avoided crossings between the Heitler-London configurations  $H(1s) + H(nl)$  and the ionic configurations  $H^+ - H^-(1s^2)$ . Particularly the  $7^1\Sigma_g^+$  state possesses a very

broad and deep ( $0.015473a.u.$ !) outer potential well which is separated by a broad barrier from the inner well located at  $R \approx 2a.u.$ . The outer minimum is located at  $R \approx 33.7a.u.$ . A series of avoided crossings at very large internuclear distances  $R \approx 300a.u.$  leads to the energetically equal dissociation limits  $H(1s) + H(4l)$  of the  $n^1\Sigma_g^+, n = 7 - 9$  states. The dissociation channel of the  $10^1\Sigma_g^+$  state is the ionic configuration  $H^+ + H^-(1s^2)$ . Tables 1 to 3 contain (among the data in the presence of a magnetic field) the total and dissociation energies at the equilibrium internuclear distances, the equilibrium internuclear distances and the total energies in the dissociation limit for the first to third excited  $^1\Sigma_g^+, n = 2 - 4$  states in the absence of the magnetic field.

## 2. Evolution in the presence of a magnetic field

The subspace of  $^1\Sigma_g$  symmetry contains the electronic ground state of the hydrogen molecule in field-free space and in the presence of a magnetic field in the regime  $0 < B < 0.1a.u.$  For a detailed discussion of the appearance of this state and the global ground state with increasing field strength in general we refer the reader to refs. [24, 25, 27–30] (see also introduction of the present work). In the following we investigate the evolution of the excited  $n^1\Sigma_g, n = 2 - 8$  states with increasing magnetic field strength for the regime  $0 < B < 100a.u.$ . We will first study the changes of the PECs of individual states with increasing field strength and thereafter we present a global view of the evolution of the spectrum. In order to compare the PECs for the same state for different field strengths we subtract from the total energies the corresponding energies in the dissociation limit (which is different for different field strengths), i.e. we show the quantity  $E(R) = E_t(R) - \lim_{R \rightarrow \infty} E_t(R)$ . In general the dissociation limit of a certain state of  $\Sigma$  symmetry changes with increasing field strength which is due to the reordering of the energy levels of the atoms (hydrogen, hydrogen negative ion) in the external field. For the atomic states we will use in the following the notation  $nm_a^{\pi_a}$  where  $n$  specifies the degree of excitation and  $m_a, \pi_a$  the atomic magnetic quantum number and z-parity, respectively.

Let us begin our investigation of the evolution of individual states with increasing field strength with the  $2^1\Sigma_g$  state whose PECs are shown in Figure 2a. The positions of the two minima and the corresponding maximum decrease with increasing field strength. The depth of the inner potential well decreases for  $B \lesssim 0.5a.u.$  and increases rapidly for  $B \gtrsim 1a.u.$ . The depth of the outer well is monotonically increasing for the complete regime  $0 < B < 100a.u.$ . For  $B \lesssim 0.01a.u.$  and  $B \gtrsim 50a.u.$  the inner well is therefore deeper than the outer well and vice versa for  $0.05 \lesssim B \lesssim 20.0a.u.$  (see figure 2a). The dissociative behaviour of the PECs changes significantly with increasing field strength. The origin of these changes is the fact that for  $B \lesssim 10a.u.$  the dissociation channel is  $H_2 \rightarrow H(10^+) + H(10^-)$  whereas for  $B \gtrsim 20a.u.$  we have the asymptotic behaviour  $H_2 \rightarrow H^+ + H^-(10_s^+)$  (the index  $s$  stands for spin singlet). The appearance of the ionic configuration as the dissociation channel for the low-lying electronic  $2^1\Sigma_g$  state can be explained as follows. It is well-known that the hydrogen negative ion possesses infinitely many bound states in the presence of a magnetic field of arbitrary strength assuming an infinite nuclear mass [44, 45]. Certain of these bound states show a monotonically increasing binding energy with increasing field strength. The latter surpass then more and more of the energy levels belonging to two hydrogen atoms one being in the global ground state and the other one in the corresponding excited state. For a sufficiently strong magnetic field we therefore expect the configuration  $H^+ + H^-(10_s^+)$  to become the dissociation channel particularly for the first excited state of  $^1\Sigma_g$  symmetry. Due to the long range forces the onset of the asymptotic ( $R \rightarrow \infty$ ) behaviour of the corresponding PECs with the ionic channel ( $H^+ + H^-$ ) is qualitatively different from the PECs with a neutral dissociation limit ( $H + H$ ). This explains the different asymptotic behaviour of the PECs shown in figure 2a with increasing field strength. Finalizing the discussion of the  $2^1\Sigma_g$  state we remark that its PECs possesses a second maximum for  $0.01 \lesssim B \lesssim 5.0a.u.$  which however occurs at large internuclear distances ( $R \approx 20a.u.$ ) and is only of the order of  $10^{-4}a.u.$  above the dissociation limit. Table 1 contains relevant data of the PECs of the  $2^1\Sigma_g$  state with increasing field strength.

Next we turn to the second excited i.e. the  $3^1\Sigma_g$  state whose PECs are shown in figure 2b. The positions of the two minima and the corresponding maximum already present in field-free space decrease monotonically with increasing field strength. Starting from  $B = 0a.u.$  the depth of the inner well decreases with increasing field strength whereas it increases for  $B \gtrsim 0.5a.u.$ . Besides a very small interval of field strengths the depth of the outer well increases with increasing field strength. For  $B < 5.0a.u.$  the outer well is deeper than the inner one whereas for  $B \gtrsim 10a.u.$  the deep inner well dominates the shape of the PEC. We remark that the curvature at the (first) maximum and the outer minimum increases significantly with increasing field strength. The evolution of these increasingly sharper turns can only be fully understood if one looks at the complete spectrum (see figure 3 and in particular 3(e)) with increasing field strength: they develop due to a number of narrow avoided crossing of the first to third excited states in strong fields. An interesting property of the PEC of the  $3^1\Sigma_g$  state is the existence of an additional outer (third) minimum for the interval  $0.01 \lesssim B \lesssim 10a.u.$  which is shown in figure 2c. This minimum arises due to the interaction with the ionic configuration  $H^+ + H^-$ . In field-free space the lowest and only bound ionic channel  $H^+ + H^-(10_s^+)$  is the dissociation channel of the  $10^1\Sigma_g^+$  state. With increasing field strength the hydrogen negative ion becomes

increasingly stronger bound (see discussion above) and therefore it occurs as the dissociation channel for the sequence of excited states  $9^1\Sigma_g, 8^1\Sigma_g, \dots$  finally becoming the dissociation channel of the  $2^1\Sigma_g$  state for  $B \gtrsim 20a.u.$ . The existence of the additional outer minimum becomes now understandable: due to the energetical lowering of the ionic dissociation channel with increasing field strength the higher excited states of  $^1\Sigma_g$  symmetry evolve outer minima and corresponding wells for certain regimes of the field strength. For the  $3^1\Sigma_g$  state this outer well is extremely shallow for  $B \lesssim 0.05a.u.$  and therefore almost invisible in figure 2c. For  $B \gtrsim 0.1a.u.$  it becomes however well-pronounced. Between  $B = 0.5a.u.$  and  $B = 1.0a.u.$  there occurs a change with respect to the dissociation channel of the  $3^1\Sigma_g$ . For  $0 < B \lesssim 0.5a.u.$  the dissociation channel is  $H(10^+) + H(20^+)$  and for  $1.0 \lesssim B \lesssim 10a.u.$  it is  $H^+ + H^-(0_s^+)$ . The similar asymptotic behaviour of the PECs belonging to different field strengths (see figure 2c for  $B = 1.0, 5.0$  and  $10.0$ ) arises due to the fact that they possess all the ionic dissociation channel. In the latter regime the position of the (third) outer minimum increases with increasing field strength (for  $B = 10.0a.u.$  the outer minimum is located at  $\approx 85a.u.$ ). Finally there is a second change of the dissociation channel of the  $3^1\Sigma_g$  state to  $H(10^+) + H(10^-)$  and therefore the outer minimum disappears for  $B \gtrsim 20a.u.$ . Table 2 contains the total and dissociation energies at the equilibrium internuclear distances, the equilibrium internuclear distances and the total energies in the dissociation limit for the second excited  $3^1\Sigma_g^+$  state in the regime  $0 < B < 100a.u.$

Next we focus on the third excited  $4^1\Sigma_g$  whose PECs with increasing field strength are shown in figure 2d. In field-free space it possesses two minima and associated potential wells located at  $R = 1.97a.u.$  and  $R = 11.21a.u.$ , respectively. The position of the inner minimum increases with increasing field strength whereas the corresponding dissociation energy decreases. Finally for  $B \approx 0.2a.u.$  the associated well disappears but reappears for  $B \gtrsim 0.5a.u.$ . With further increasing field strength the position of this inner minimum decreases and the depth of the corresponding well increases monotonically for  $B \gtrsim 1a.u.$ . Independently of this first inner minimum and the outer minimum there appears for  $B \gtrsim 0.2a.u.$  an additional third minimum and corresponding well (see table 3 and figure 2d) for small internuclear distances  $1 - 3a.u.$ . Although this new minimum and well are energetically well below the dissociation limit for  $B \gtrsim 20.0a.u.$  they are separated from the other inner minimum only by a tiny barrier. These facts will become better understandable in the context of our discussion of the evolution of the whole spectrum with increasing field strength (see below). The properties of the PEC of the  $4^1\Sigma_g$  state at large internuclear distances are somewhat analogous to that of the  $3^1\Sigma_g$  state. The outer minimum has its origin in the interaction of the neutral  $H + H$  and ionic  $H^+ + H^-$  configurations. Starting with  $B = 0$  and increasing the field strength the depth of the outer well increases. The first change of the dissociation channel from  $H_2 \rightarrow H(10^+) + H(30^+)$  to  $H_2 \rightarrow H^+ + H^-(10_s^+)$  occurs in the regime  $0.1 < B < 0.2a.u.$ . In the regime  $0.1 \lesssim B \lesssim 1.0a.u.$  the position of the outer minimum increases with increasing field strength (for  $B = 0.5a.u.$  it is already  $R = 50a.u.$ ) and the depth of the outer well decreases. Due to the further increasing binding energy of the hydrogen negative ion  $10_s^+$  state with increasing field strength we encounter a second change of the dissociation channel at  $B \approx 1.0a.u.$  to  $H_2 \rightarrow H(10^+) + H(20^+)$  which causes the disappearance of the outer minimum and well. Table 3 provides the corresponding data for the  $4^1\Sigma_g$  state.

The PECs of the  $5^1\Sigma_g$  and  $6^1\Sigma_g$  states are shown in figures 2e and 2f, respectively. For both states the positions of the maxima and minima as well as the corresponding total energies show an 'irregular' behaviour as a function of the field strength for  $B \lesssim 2.0a.u.$ . We therefore focus on the main features of these states. For certain regimes of the field strength we observe double well structures for the PECs. Analogously to the  $n^1\Sigma_g, n = 2 - 4$  states there exist additional outer minima and wells due to the interaction with the ionic configuration for certain field strength regimes. For  $B > 2.0a.u.$  the position of the first inner minimum decreases rapidly with increasing field strength whereas the corresponding dissociation energy increases. Also we observe the existence of minima whose energies lie above the dissociation energy, i.e. the corresponding wells contain if at all metastable states. We remark that some of the above-discussed features, in particular those associated with small energy scales, might not be visible in the corresponding figures 2 but only in a zoom of the relevant regimes of internuclear distances of the considered PECs. We again emphasize that due to the large amount of data we do not present full PECs or data on the higher excited states  $n^1\Sigma_g, n = 5 - 8$  which can be obtained from the authors upon request.

### 3. Discussion of the evolution of the complete spectrum

In the present subsection we focus on the evolution of the complete spectrum of the excited  $n^1\Sigma_g, n = 2 - 8$  states with increasing field strength. This will give us the complementary information to the evolution of individual states presented above. Figure 3a-f shows the corresponding PECs for the field strengths  $B = 0.01, 0.1, 0.5, 5.0, 100.0a.u.$ , respectively. The PECs of the five energetical lowest excited states  $n^1\Sigma_g, n = 2 - 6$  are hereby illustrated with full lines indicating their higher accuracy whereas the PECs of the electronic states  $n^1\Sigma_g, n = 7, 8$  are less accurate and illustrated with dotted lines. Before we discuss the evolution with increasing field strength some general remarks are in order. The energy gap between the ground state  $1^1\Sigma_g$  and the first excited state  $2^1\Sigma_g$  is of the order of  $0.4a.u.$  in

field-free space and increases monotonically with increasing field strength. At the same time the total energies of all states  $n^1\Sigma_g$  are shifted in lowest order proportional to  $B$  with increasing field strength which is due to the raise of the kinetic energy in the presence of a magnetic field.

In field-free space many of the dissociation channels of the PECs of excited  $^1\Sigma_g$  states are degenerate due to the degeneracies of the field-free hydrogen atom (see figure 1 and 4). The major difference of the PECs in field-free space compared to those for weak fields is the removal of these degeneracies (see, for example, figure 3a for  $B = 0.01a.u.$ ). With increasing field strength figures 3a-d ( $B = 0.01, 0.1, 0.5$  and  $5.0a.u.$ ) demonstrate the systematic lowering of the diabatic energy curve belonging to the ionic configuration  $H^+ + H^-(1s^2)$ . This diabatic curve passes through the spectrum with increasing field strength thereby causing an intriguing evolution of avoided crossings and corresponding potential wells for the individual states. At  $B \approx 0.1a.u.$  the fourth excited  $5^1\Sigma_g$  state acquires the ionic dissociation channel. The  $7^1\Sigma_g$  state thereby loses its outer potential well which was very well-pronounced in the absence of the external field. In the same course the  $3^1\Sigma_g$  state shows a number of avoided crossings with the  $2^1\Sigma_g$  state: it develops an additional outer minimum and well which is rather deep at  $B \approx 0.5a.u.$  accompanied by the flattening of the first inner well and the deepening of the second inner well. Furthermore we observe for  $B \approx 0.5a.u.$  the appearance of a large number of avoided crossings among the higher excited states  $n^1\Sigma_g, n = 5 - 8$  at  $R \approx 5a.u.$ . At  $B \approx 0.2a.u.$  the third excited  $4^1\Sigma_g$  state acquires the ionic dissociation channel. Subsequently, i.e. with further increasing field strength, the second excited  $3^1\Sigma_g$  state (see figure 3d) and finally the first excited  $2^1\Sigma_g$  state acquire ionic character for sufficiently large internuclear distances. In the high field situation (see figure 3e for  $B = 100a.u.$ ) only the energetically lowest excited state possess a well-pronounced double well structure and the overall picture is dominated by the fact that the PECs of the considered states possess a very similar shape and are energetically very close to each other in particular around the inner minimum at small internuclear distances. Figure 3f shows for  $B = 100a.u.$  a zoom of the series of avoided crossings occurring for the higher excited states  $n^1\Sigma_g, n = 5 - 10$  in the regime  $2 < R < 12a.u.$ .

## B. Excited ungerade singlet states

### 1. Field-free states

The four energetically lowest states of  $^1\Sigma_u^+$  symmetry at  $B = 0$  have been investigated in detail and with high accuracy in the literature [42]. Our results [39] show a relative accuracy of  $10^{-4}$  for the energies of the  $1^1\Sigma_u^+$  state and of  $10^{-5}$  for the first two excited states i.e. the  $n^1\Sigma_u^+, n = 2, 3$  states. The energies of the  $4^1\Sigma_u^+$  state are significantly lower than the data presented in [42]. The PECs for the  $n^1\Sigma_u^+, n = 4 - 9$  presented in ref. [39] for the first time are estimated to possess an accuracy of  $10^{-5}$  for the  $n^1\Sigma_u^+, n = 4 - 6$  states and  $10^{-4}$  for the  $n^1\Sigma_u^+, n = 7 - 9$  states. Figure 4 shows the PECs of the ground as well as eight excited states of  $^1\Sigma_u^+$  symmetry in the range  $1 < R < 1000a.u.$  on a logarithmic scale.

The PEC of the ground state  $1^1\Sigma_u^+$  of ungerade symmetry possesses a minimum at  $R = 2.43a.u.$  and a corresponding deep well. A closer look at the wave function reveals its ionic character for  $3 < R < 7a.u.$ . With further increasing internuclear distance the ionic character of the wave function decreases and the corresponding dissociation channel is  $H_2 \rightarrow H(1s) + H(2p)$ . The PEC of the first excited  $2^1\Sigma_u^+$  state is similar to that of the ground state  $1^1\Sigma_u^+$ : its equilibrium internuclear distance is  $R_{eq} = 2.09$  the dissociation channel is identical to that of the  $1^1\Sigma_u^+$  state. The depth of its single well is however only one third of the depth of the well of the  $1^1\Sigma_u^+$  state. For the higher excited states we observe a similar behaviour as in the case of the excited electronic states of  $^1\Sigma_g^+$  symmetry. The PECs of the  $n^1\Sigma_u^+, n = 3 - 9$  states possess a deep well around a minimum located approximately at  $R \approx 2a.u.$ . Furthermore the  $n^1\Sigma_u^+, n = 3, 6$  states exhibit additional deep outer potential wells at large internuclear distances which arise due to the avoided crossings of the Heitler-London configurations with the corresponding ionic configuration. The outer minimum of the  $6^1\Sigma_u^+$  state is located at  $33.7a.u.$  and the corresponding well possesses a remarkable depth of  $0.015134a.u.$ : it is expected to contain a large number of long-lived vibrational states. Tables 4 to 6 contain (among the data in the presence of the magnetic field) the total and dissociation energies at the equilibrium internuclear distances, the equilibrium internuclear distances and the total energies in the dissociation limit for the first to third excited  $^1\Sigma_u^+$  states in the absence of the magnetic field.

### 2. Evolution in the presence of a magnetic field

First of all we remark that the dissociation channels of the  $(n + 1)^1\Sigma_g$  states coincide with those of the  $n^1\Sigma_u$  states for  $n = 1 - 7$  in the complete regime  $0 \leq B \leq 100a.u.$ . The qualitative behaviour of the PECs of the  $n^1\Sigma_u$  states at

large internuclear distances is therefore similar to that of the  $(n+1)^1\Sigma_g$  states discussed in the previous section. In particular many of the explanations and remarks provided there hold also for the present case of the  $n^1\Sigma_u$  states.

Before discussing the behaviour of the PECs of the individual excited  $n^1\Sigma_u$  states with increasing field strength some remarks concerning the lowest, i.e. ground state of  $^1\Sigma_u$  symmetry are in order (for its PEC with increasing field strength see figure 6). Its dissociation energy increases monotonically with increasing field strength whereas its equilibrium internuclear distance increases slightly for weak fields and decreases significantly for increasingly stronger fields. As indicated above the asymptotic  $R \rightarrow \infty$  behaviour of the PECs of the  $1^1\Sigma_u$  and  $2^1\Sigma_g$  states is very similar. For  $B = 100a.u.$  the PEC of the  $1^1\Sigma_u$  state possesses a peculiar shape which is largely determined by the ionic dissociation channel  $H^+ + H^-(10_s^+)$  (see figure 6f). For more details on this state we refer the reader to ref. [27,28].

The first excited  $2^1\Sigma_u$  state possesses in field-free space an equilibrium internuclear distance  $R_{eq} = 2.09a.u.$ . Figure 5a shows the corresponding PEC with increasing field strength for  $0 \leq R \leq 5a.u.$  whereas figure 5b illustrates particularly the behaviour at large internuclear distances. In the regime  $0 \leq B \lesssim 0.2a.u.$  the dissociation energy decreases slightly and the bond length increases. With further increasing field strength the dissociation energy increases drastically and the bond length decreases. For  $0.1 \lesssim B \lesssim 50a.u.$  there exists a maximum and a corresponding additional outer minimum at large internuclear distances (see figure 5b) whose origin is again the emergence of the ionic configuration for the wave function of the  $2^1\Sigma_u$  state. Figure 5b also demonstrates the similarity of the asymptotic  $R \rightarrow \infty$  behaviour of the PECs of the  $2^1\Sigma_u$  state in the regime  $1.0 \leq B \leq 10.0a.u.$ . The corresponding data for the PECs of the first excited  $2^1\Sigma_u$  state are given in table 4.

Turning to the second excited  $3^1\Sigma_u$  state we observe that the depth of the potential well located for  $B = 0a.u.$  at  $R_{eq} = 2.03a.u.$  decreases for weak fields whereas it increases significantly for strong fields  $B \gtrsim 1.0a.u.$  (see figure 5c). The existence of an additional outer minimum for this state can be seen in figure 5d. In many respects a similar behaviour to that of the  $2^1\Sigma_u$  state is observed although, of course, the regimes of field strength for which the individual phenomena take place are different. Table 5 contains the corresponding data of the PECs of the  $3^1\Sigma_u$  state. Finally figures 5e and 5f show the PECs of the  $n^1\Sigma_u, n = 4, 5$  states with increasing field strength, respectively. They exhibit a number of maxima and minima most of which can however hardly be seen in figures 5e,f or occur at large internuclear distances. The origin of their existence are again the different (ionic and neutral) dissociation channels. These maxima and minima are present only for certain individually different regimes of the field strength. Some of them are located above and some of them below the dissociative threshold. As can be seen the bond length (belonging to the inner minimum) decreases monotonically and the dissociation energy increases significantly above some critical value  $B_c$ . The inner minimum and associated well possesses a remarkably large dissociation energy for strong fields. Table 6 provides data on the PECs of the  $4^1\Sigma_u$  state.

To finalize our discussion on the  $^1\Sigma_u$  subspace we show in figure 6 the evolution of the spectrum with increasing field strength. Figures 6a-f show the PECs for the  $n^1\Sigma_u, n = 1 - 8$  states for the field strengths  $B = 0.05, 0.1, 0.5, 1.0, 10.0, 100.0a.u.$ , respectively. Analogously to the case of the  $^1\Sigma_g$  subspace we observe for weak fields the removal of the degeneracies due to the field-free hydrogen atom in the dissociation limit. With increasing field strength we see the lowering of the diabatic energy line belonging to the ionic configuration which causes the appearance and disappearance of outer maxima, minima and corresponding outer potential wells until finally ( $B = 100a.u.$ ) the  $1^1\Sigma_u$  state possess the ionic dissociation channel  $H_2 \rightarrow H^+ + H^-(10_s^+)$  which is the origin of the peculiar shape of its PEC. A number of further observations made for the manifold of the  $n^1\Sigma_g, n = 1 - 8$  states above can also be seen for the  $n^1\Sigma_u, n = 1 - 8$  states in figure 6 like, for example, the similar shape of the potential wells of the excited states in the high field limit.

#### IV. CONCLUSIONS

The hydrogen molecule is the most fundamental molecular system and of immediate importance in a variety of different physical circumstances. In spite of the fact that it has been investigated over the past decades in great detail and that our knowledge on this system has grown enormously there are plenty of questions and problems to be addressed even for the molecule in field-free space. As an example we mention certain highly excited Rydberg states ( $7^1\Sigma_g^+, 6^1\Sigma_u^+$ ) which, due to the ionic character of the binding for certain regimes of the internuclear distance, possesses a deep outer well at large distances which contains a considerable number of vibrational states. On the other hand the detailed knowledge of hydrogen (even of highly excited states) is of utmost importance for our understanding and interpretation of the astrophysically observed interstellar radiation.

Much less is known about the behaviour of the hydrogen molecule in strong magnetic fields. With increasing field strength the ground state of the molecule undergoes two transitions which are due to a change of the spin and orbital character, respectively. Very recently the global ground state configurations have been identified for the parallel configuration (there are good reasons which lead to the conjecture that the derived results hold for arbitrary

angle of the internuclear and magnetic field axis) both on the Hartree-Fock level [29, 30] and via a fully correlated approach [27, 28]. For low fields the ground state is of spin singlet  $^1\Sigma_g$  symmetry, for intermediate fields the spin triplet  $^3\Sigma_u$  state represent the ground state whereas in the high field regime the  $^3\Pi_u$  state is the energetically lowest state.

The present work goes for the first time beyond the ground state properties and investigates excited states of the hydrogen molecule in the broad regime  $0 < B < 100a.u.$ . We hereby focus on singlet states of both gerade as well as ungerade symmetry: up to seven excited states have been studied for the parallel configuration with a high accuracy of the obtained PECs. A variety of different phenomena have been observed out of which we mention here only the most important ones. Double well structures observed in particular for the field-free  $n^1\Sigma_g^+$  states are severely modified in the presence of the field thereby showing a 'coming and going' of new maxima and minima as well as corresponding wells. The overall tendency in the strong field limit is the development of deep inner wells containing a large number of vibrational states. In the course of the increasing field strength a fundamental phenomenon occurs which has a strong impact on the overall shape of the PECs. Due to the fact that the hydrogen negative ion becomes increasingly bound with increasing field strength we encounter changes in the dissociation channels of individual states from neutral  $H_2 \rightarrow H + H^*$  to ionic  $H_2 \rightarrow H^+ + H^-$  character. For a certain regime of field strength  $B_{c1} < B < B_{c2}$  a certain excited state possesses therefore the ionic dissociation channel thereby modifying the asymptotic behaviour of its PEC to an attractive Coulombic tail. For weaker fields  $B < B_{c1}$  higher excited states possess this ionic dissociation channel whereas for stronger fields  $B > B_{c2}$  it belongs to increasingly lower excitations. These facts influence the overall appearance of the spectrum thereby creating features like outer potential wells and/or largely changing avoided crossings.

The data on the PECs of the excited singlet states obtained here should serve as part of the material to be accumulated for the investigation of quasimolecular absorption features in magnetic white dwarfs. The investigation of excited triplet states of  $\Sigma$  symmetry or of  $\Pi$  states, which are of equal importance, are left to future investigations.

## V. ACKNOWLEDGMENT

Fruitful discussions with W.Becken are gratefully acknowledged. The Deutsche Forschungsgemeinschaft is gratefully acknowledged for financial support.

- 
- [1] H.Friedrich and D.Wintgen, Phys.Rep. **183**, 37 (1989)
  - [2] H. Ruder, G. Wunner, H. Herold und F. Geyer, Atoms in Strong Magnetic Fields, Springer Verlag A&A 1994.
  - [3] Atoms and Molecules in Strong External Fields, Plenum Press New York (1998), ed. by P.Schmelcher and W.Schweizer
  - [4] H. Forster, W. Strupat, W. Rösner, G. Wunner, H. Ruder, H. Herold, J.Phys.B **17**, 1301 (1984)
  - [5] R.J.W. Henry, R.F. O'Connell, Astrophys.J. **282**, L97 (1984)
  - [6] D.T. Wickramasinghe, L. Ferrario, Astrophys. J.**327**, 222 (1988)
  - [7] S. Jordan, Lecture Notes in Physics **328**, 333 Springer (1989)
  - [8] S. Jordan, P. Schmelcher, W. Becken and W. Schweizer, Astron.& Astrophys. **336** L33-L36 (1998)
  - [9] W. Becken, P. Schmelcher and F.K. Diakonov, J. Phys.B **32**, 1557 (1999)
  - [10] W. Becken and P. Schmelcher, subm.to J. Phys.B
  - [11] D. Reimers, S. Jordan, V. Beckmann, N. Christlieb, L. Wisotzki, Astr.& Astrophys. **337** (1998) L13
  - [12] S. Jordan, private communication
  - [13] U. Wille, Phys. Rev. A **38**, 3210 (1988).
  - [14] U. Kappes and P. Schmelcher, Phys. Rev. A **53**, 3869 (1996).
  - [15] U. Kappes and P. Schmelcher, Phys. Rev. A **54**, 1313 (1996).
  - [16] U. Kappes and P. Schmelcher, Phys. Lett. A **210**, 409 (1996).
  - [17] Yu. P. Kravchenko and M. A. Liberman, Phys. Rev. A **55**, 2701 (1997).
  - [18] U. Kappes, P. Schmelcher, and T. Pacher, Phys. Rev. A **50**, 3775 (1994).
  - [19] U. Kappes and P. Schmelcher, Phys. Rev. A **51**, 4542 (1995).
  - [20] T. S. Monteiro and K. T. Taylor, J. Phys. B **23**, 427 (1990).
  - [21] S. Basile, F. Trombetta, and G. Ferrante, Nuovo Cimento **9**, 457 (1987).
  - [22] A. V. Turbiner, Pis'ma Zh. Eksp. Teor. Fiz. **38**, 510 (1983), [JETP Lett. **38**, 618 (1983)].
  - [23] A. V. Korolev and M. A. Liberman, Phys. Rev. A **45**, 1762 (1992).
  - [24] D. Lai, E. E. Salpeter, and S. L. Shapiro, Phys. Rev. A **45**, 4832 (1992).

- [25] G. Ortiz, M. D. Jones, and D. M. Ceperley, Phys. Rev. A **52**, R3405 (1995).
- [26] D. Lai and E. E. Salpeter, Phys. Rev. A **53**, 152 (1996).
- [27] T. Detmer, P. Schmelcher, F. K. Diakonov, and L. S. Cederbaum, Phys. Rev. A **56**, 1825 (1997)
- [28] T. Detmer, P. Schmelcher, and L. S. Cederbaum, Phys. Rev. A **57**, 1767 (1998)
- [29] Yu. P. Kravchenko and M.A. Liberman, Phys.Rev. A **56**, R2510 (1997)
- [30] Yu. P. Kravchenko and M.A. Liberman, Phys.Rev. A **57**, 3403 (1998)
- [31] P. Schmelcher and L. S. Cederbaum, Phys. Rev. A **41**, 4936 (1990).
- [32] B. Johnson, J. Hirschfelder, and K. Yang, Rev. Mod. Phys. **55**, 109 (1983).
- [33] J. E. Avron, I. W. Herbst, and B. Simon, Ann. Phys. **114**, 431 (1978).
- [34] P. Schmelcher, L. S. Cederbaum, and H.-D. Meyer, Phys. Rev. A **38**, 6066 (1988).
- [35] P. Schmelcher, L. S. Cederbaum, and U. Kappes, in "Conceptual Trends in Quantum Chemistry", edited by Eugene S. Kryachko (Kluwer Academic Publishers, Dordrecht, 1994).
- [36] P. Schmelcher, L. S. Cederbaum, and H.-D. Meyer, J. Phys. B **21**, L445 (1988).
- [37] P. Schmelcher and L. S. Cederbaum, Phys. Rev. A **37**, 672 (1988).
- [38] U. Kappes and P. Schmelcher, J. Chem. Phys. **100**, 2878 (1994).
- [39] T. Detmer, P. Schmelcher and L.S. Cederbaum, J.Chem.Phys. **109**, 9694 (1998)
- [40] L.Wolniewicz, J.Chem.Phys.**99**, 1851 (1993);J.Chem.Phys.**108**, 1499 (1998)
- [41] E.Reinhold, W.Hogervorst and W.Ubachs, Phys.Rev.Lett.**78**, 2543 (1997)
- [42] K.Dressler and L.Wolniewicz, Ber.Bunsenge.Phys.Chem.**99**, 246 (1995)
- [43] W.Kolos and L.Wolniewicz, J.Chem.Phys.**45**, 509 (1966)
- [44] J.E. Avron, I.W. Herbst and B. Simon, Commun. Math. Phys. **79**, 529 (1981)
- [45] V.G.Bezchastnov, P.Schmelcher and L.S.Cederbaum, subm.f.publ.

## FIGURE CAPTIONS

**Figure 1:** The potential energy curves of the excited  $n^1\Sigma_g^+$ ,  $n = 2 - 9$  electronic states of the hydrogen molecule in the absence of a magnetic field.

**Figure 2:** The evolution of the potential energy curves for some excited  $^1\Sigma_g$  electronic states of the hydrogen molecule in the presence of a magnetic field  $0 < B < 100a.u.$ . In detail are shown the evolution of the PECs for the (a)  $2^1\Sigma_g$ , (b)  $3^1\Sigma_g$ , (c) zoom of  $3^1\Sigma_g$ , (d)  $4^1\Sigma_g$ , (e)  $5^1\Sigma_g$  and (f)  $6^1\Sigma_g$  states, respectively. Shown is the quantity  $E(R) = E_t(R) - \lim_{R \rightarrow \infty} E_t(R)$  where  $E_t(R)$  is the total energy.

**Figure 3:** The spectrum of potential energy curves for the excited  $n^1\Sigma_g$ ,  $n = 2 - 8$  electronic states of the hydrogen molecule in the presence of a magnetic field  $0 < B < 100a.u.$  with increasing field strength. In detail are shown the PECs for (a)  $B = 0.01$  (b)  $B = 0.1$  (c)  $B = 0.5$  (d)  $B = 5.0$  (e)  $B = 100.0$  and (f) zoom of  $B = 100.0a.u.$ , respectively.

**Figure 4:** The potential energy curves of the excited  $n^1\Sigma_u^+$ ,  $n = 1 - 9$  electronic states of the hydrogen molecule in the absence of a magnetic field.

**Figure 5:** The evolution of the potential energy curves for some excited  $^1\Sigma_u$  electronic states of the hydrogen molecule in the presence of a magnetic field  $0 < B < 100a.u.$ . In detail are shown the evolution of the PECs for the (a)  $2^1\Sigma_g$ , (b) zoom of  $2^1\Sigma_g$ , (c)  $3^1\Sigma_g$ , (d) zoom of  $3^1\Sigma_g$ , (e)  $4^1\Sigma_g$  and (f)  $5^1\Sigma_g$  states, respectively. Shown is the quantity  $E(R) = E_t(R) - \lim_{R \rightarrow \infty} E_t(R)$  where  $E_t(R)$  is the total energy.

**Figure 6:** The spectrum of potential energy curves for the excited  $n^1\Sigma_u$ ,  $n = 1 - 8$  electronic states of the hydrogen molecule in the presence of a magnetic field  $0 < B < 100a.u.$  with increasing field strength. In detail are shown the PECs for (a)  $B = 0.05$  (b)  $B = 0.1$  (c)  $B = 0.5$  (d)  $B = 1.0$  (e)  $B = 10.0$  and (f)  $B = 100.0a.u.$ , respectively.

# Tables

TABLE I. Data for the first excited  $^1\Sigma_g$  state: Total energies  $E_{t1}, E_{t2}$  and dissociation energies  $E_{d1}, E_{d2}$  at the corresponding equilibrium internuclear distance, the equilibrium internuclear distances  $R_{eq1}, R_{eq2}$  and the total energy in the dissociation limit  $\lim_{R \rightarrow \infty} E_t$  as a function of the field strength  $0 \leq B \leq 100$  (all quantities are given in atomic units).

B	$R_{eq1}$	$E_{d1}$	$E_{t1}$	$R_{eq2}$	$E_{d2}$	$E_{t2}$	$\lim_{R \rightarrow \infty} E_{tot}$
0.0	1.91	0.093122	-0.718121	4.39	0.089241	-0.714240	-0.624999
0.001	1.91	0.093120	-0.718117	4.39	0.089242	-0.714239	-0.624997
0.005	1.91	0.093061	-0.718017	4.39	0.089252	-0.714208	-0.624956
0.01	1.91	0.092878	-0.717703	4.39	0.089289	-0.714114	-0.624825
0.05	1.90	0.087831	-0.708672	4.39	0.090459	-0.711300	-0.620841
0.1	1.88	0.077017	-0.686953	4.38	0.093325	-0.703261	-0.609936
0.2	1.88	0.057630	-0.633195	4.33	0.100709	-0.676274	-0.575565
0.5	1.89	0.040502	-0.462472	4.08	0.122427	-0.544397	-0.421970
1.0	1.78	0.044819	-0.135993	3.76	0.150618	-0.241792	-0.091174
2.0	1.54	0.067740	0.612336	3.37	0.191218	0.488858	0.680076
5.0	1.18	0.140991	3.130994	2.88	0.269224	3.002761	3.271985
10.0	0.95	0.245637	7.623918	2.55	0.351756	7.517799	7.869555
20.0	0.76	0.359056	16.960943	2.27	0.408351	16.911648	17.319999
50.0	0.56	0.575262	45.784366	1.96	0.471572	45.888056	46.359628
100.0	0.44	0.821768	94.614199	1.76	0.521822	94.914145	95.435967

TABLE II. Data for the second excited  $^1\Sigma_g$  state: Total energies  $E_{t1} - E_{t3}$  and dissociation energies  $E_{d1} - E_{d3}$  at the corresponding equilibrium internuclear distance, the equilibrium internuclear distances  $R_{eq1} - R_{eq3}$  and the total energy in the dissociation limit  $\lim_{R \rightarrow \infty} E_t$  as a function of the field strength  $0 \leq B \leq 100$  (all quantities are given in atomic units).

B	$R_{eq1}$	$E_{d1}$	$E_{t1}$	$R_{eq2}$	$E_{d2}$	$E_{t2}$	$R_{eq3}$	$E_{d3}$	$E_{t3}$	$\lim_{R \rightarrow \infty} E_{tot}$
0.0	2.03	0.035466	-0.660465	3.27	0.038014	-0.663013				-0.624999
0.001	2.03	0.035462	-0.660458	3.27	0.038021	-0.663017				-0.624996
0.005	2.03	0.035399	-0.660305	3.27	0.038045	-0.662951				-0.624906
0.01	2.03	0.035225	-0.659851	3.27	0.038101	-0.662727	18.97	0.000007	-0.624633	-0.624626
0.05	2.04	0.033199	-0.649592	3.20	0.040478	-0.656871	10.56	0.001510	-0.617903	-0.616393
0.1	2.03	0.030981	-0.626596	3.06	0.048089	-0.643704	10.02	0.006992	-0.602607	-0.595615
0.2	1.94	0.023894	-0.563261	2.86	0.064882	-0.604249	10.43	0.026352	-0.565719	-0.539367
0.5	1.90	0.030305	-0.378302	2.73	0.079773	-0.427788	10.69	0.066892	-0.414907	-0.348015
1.0	1.78	0.039842	-0.041327	2.50	0.091331	-0.092816	10.96	0.085978	-0.087463	-0.001485
2.0	1.54	0.042657	0.717581	2.22	0.089173	0.671065	12.14	0.079131	0.681107	0.760238
5.0	1.19	0.075290	3.248431	1.86	0.091565	3.232156	19.38	0.051644	3.272077	3.323721
10.0	0.96	0.131036	7.749942	1.63	0.093390	7.787588	85.58	0.011423	7.869555	7.880978
20.0	0.76	0.275591	17.095639	1.44	0.142076	17.229154				17.371230
50.0	0.56	0.605249	45.931209	1.22	0.250618	46.285840				46.536458
100.0	0.45	0.976059	94.770524	1.09	0.357751	95.388832				95.746583

TABLE III. Data for the third excited  $^1\Sigma_g$  state: Total energies  $E_{t1} - E_{t3}$  and dissociation energies  $E_{d1} - E_{d3}$  at the corresponding equilibrium internuclear distance, the equilibrium internuclear distances  $R_{eq1} - R_{eq3}$  and the total energy in the dissociation limit  $\lim_{R \rightarrow \infty} E_t$  as a function of the field strength  $0 \leq B \leq 100$  (all quantities are given in atomic units).

B	$R_{eq1}$	$E_{d1}$	$E_{t1}$	$R_{eq2}$	$E_{d2}$	$E_{t2}$	$R_{eq3}$	$E_{d3}$	$E_{t3}$	$\lim_{R \rightarrow \infty} E_{tot}$
0.0	1.97	0.099408	-0.654963				11.21	0.049597	-0.605152	-0.555555
0.001	1.97	0.099397	-0.654944				11.21	0.049604	-0.605151	-0.555547
0.005	1.97	0.099051	-0.654469				11.21	0.049686	-0.605104	-0.555418
0.01	1.97	0.098011	-0.653029				11.21	0.049930	-0.604948	-0.555018
0.05	1.99	0.081038	-0.625896	2.93	0.068063	-0.612921	11.39	0.055502	-0.600360	-0.544858
0.1	2.05	0.075239	-0.597699				12.04	0.06419	-0.586650	-0.522460
0.2				2.46	0.067543	-0.546109	15.62	0.059554	-0.538120	-0.478566
0.5	1.91	0.022150	-0.350029	2.35	0.035929	-0.363808	50.06	0.020138	-0.348017	-0.327879
1.0	1.77	0.019181	-0.010815	2.17	0.030750	-0.022384				0.008366
2.0	1.53	0.053756	0.750088	1.95	0.058173	0.745671				0.803844
5.0	1.19	0.142822	3.283035	1.67	0.116673	3.309184				3.425857
10.0	0.96	0.257211	7.786043	1.50	0.176832	7.866422				8.043254
20.0	0.76	0.427463	17.133303	1.34	0.249318	17.311448				17.560766
50.0	0.56	0.768452	45.971004	1.16	0.362134	46.377322				46.739456
100.0	0.45	1.142090	94.811929	1.05	0.464011	95.490008				95.954019

TABLE IV. Data for the first excited  $^1\Sigma_u$  state: Total energies  $E_{t1} E_{t2}$  and dissociation energies  $E_{d1} E_{d2}$  at the corresponding equilibrium internuclear distance, the equilibrium internuclear distances  $R_{eq1} R_{eq2}$ , the positions  $R_{max}$ , and the total energy  $E_{max}$  at the maximum, and the total energy in the dissociation limit  $\lim_{R \rightarrow \infty} E_t$  as a function of the field strength  $0 \leq B \leq 100$  (all quantities are given in atomic units).

B	$R_{eq1}$	$E_{d1}$	$E_{t1}$	$R_{eq2}$	$E_{d2}$	$E_{t2}$	$R_{max}$	$E_{max}$	$\lim_{R \rightarrow \infty} E_{tot}$
0.0	2.09	0.040772	-0.665771						-0.624999
0.001	2.08	0.040770	-0.665766						-0.624996
0.005	2.09	0.040697	-0.665603						-0.624906
0.01	2.09	0.040477	-0.665103						-0.624626
0.05	2.12	0.037068	-0.653461						-0.616393
0.1	2.13	0.036237	-0.631852	9.37	0.008169	-0.603784	5.16	-0.602345	-0.595615
0.2	2.12	0.043756	-0.583123	10.09	0.027637	-0.567004	4.60	-0.555876	-0.539367
0.5	2.03	0.065201	-0.413216	10.34	0.068386	-0.416401	4.01	-0.382377	-0.348015
1.0	1.85	0.079251	-0.080736	10.55	0.087513	-0.088998	3.66	-0.038398	-0.001485
2.0	1.59	0.085790	0.674448	11.46	0.080259	0.679979	3.34	0.744375	0.760238
5.0	1.22	0.121736	3.201985	10.49	0.052138	3.271583	2.95	3.349758	3.323721
10.0	0.98	0.178133	7.702800	9.70	0.011729	7.869204	2.69	7.955928	7.880933
20.0	0.78	0.321481	17.049749	9.27	0.000271	17.370959	2.46	17.464313	17.371230
50.0	0.57	0.646721	45.889737	9.04	0.000168	46.536290	2.21	46.635075	46.536458
100.0	0.45	1.012902	94.733681	9.04		95.746735	2.05	95.846945	95.746583

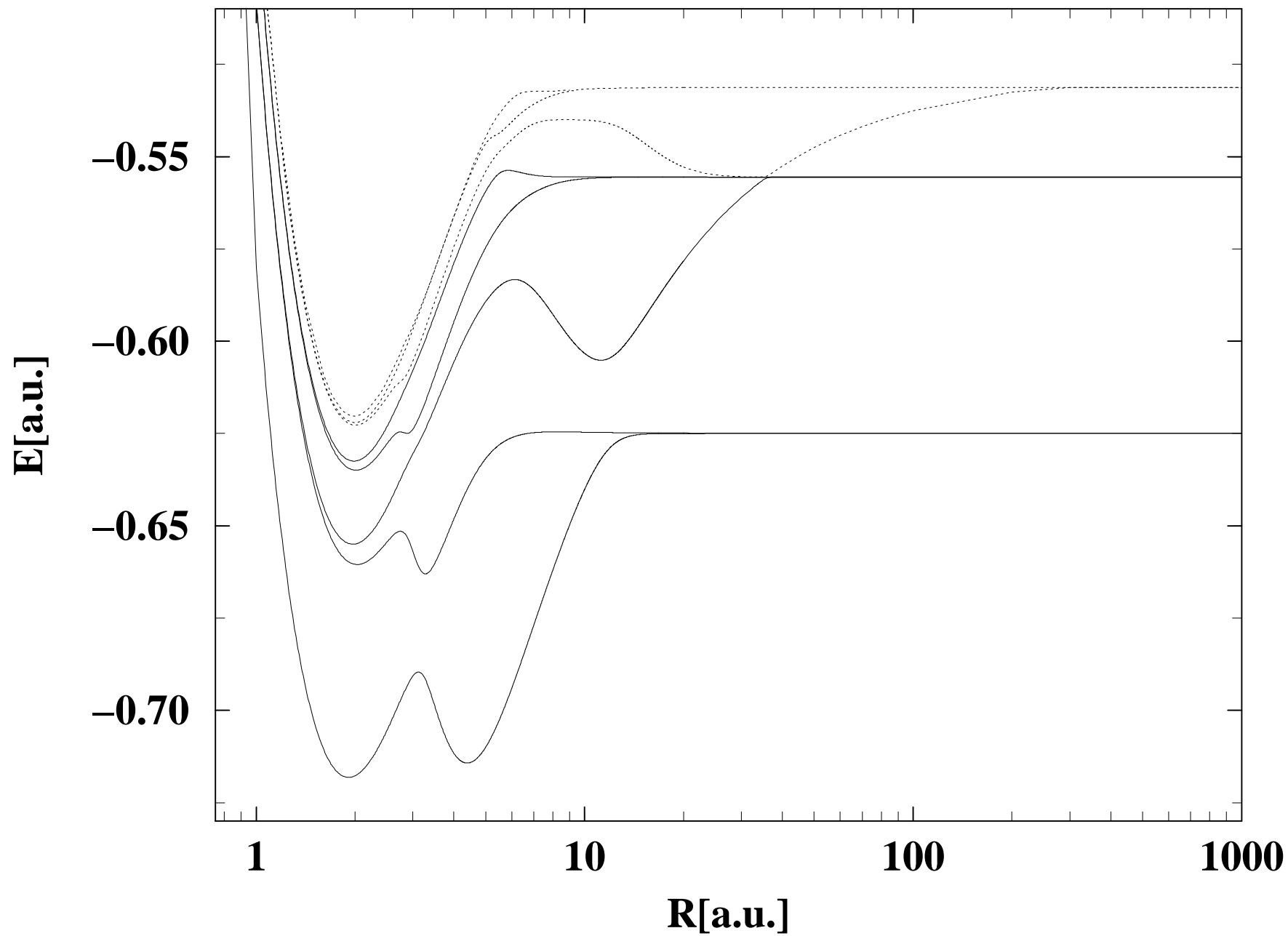
TABLE V. Data for the second excited  $^1\Sigma_u$  state: Total energies  $E_{t1}$   $E_{t2}$  and dissociation energies  $E_{d1}$   $E_{d2}$  at the corresponding equilibrium internuclear distance, the equilibrium internuclear distances  $R_{eq1}$   $R_{eq2}$ , the positions  $R_{max}$ , and the total energy  $E_{max}$  at the maximum, and the total energy in the dissociation limit  $\lim_{R \rightarrow \infty} E_t$  as a function of the field strength  $0 \leq B \leq 100$  (all quantities are given in atomic units).

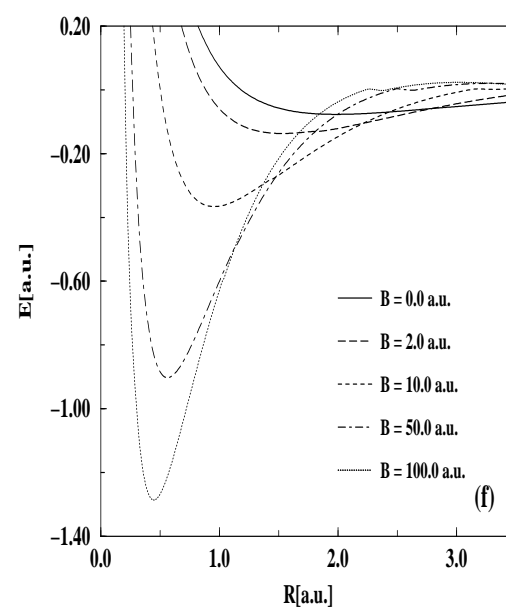
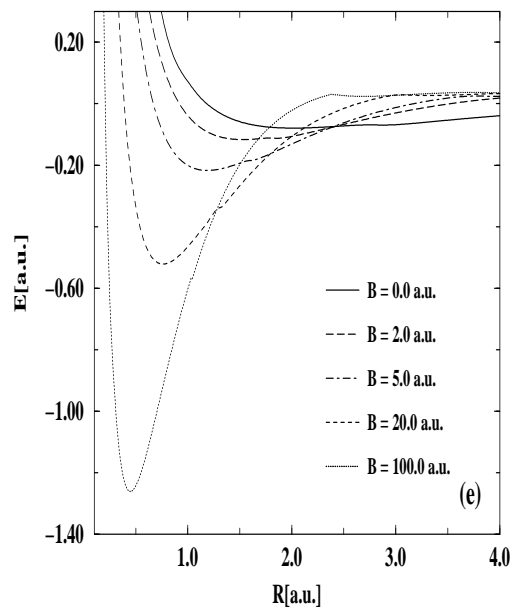
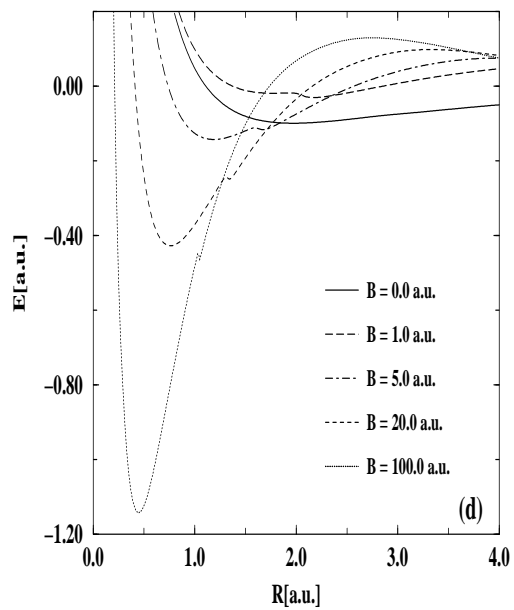
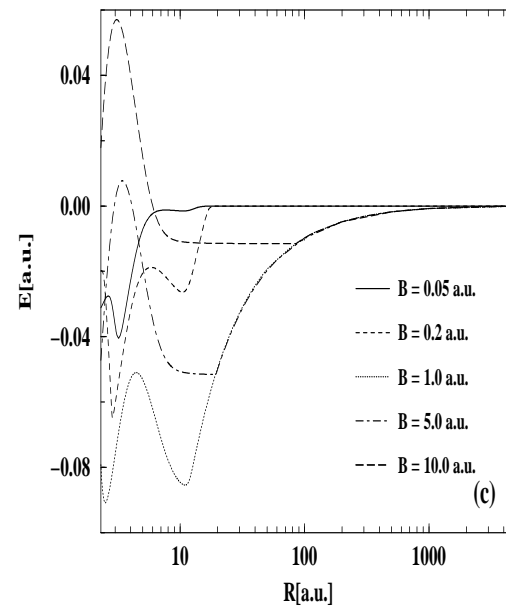
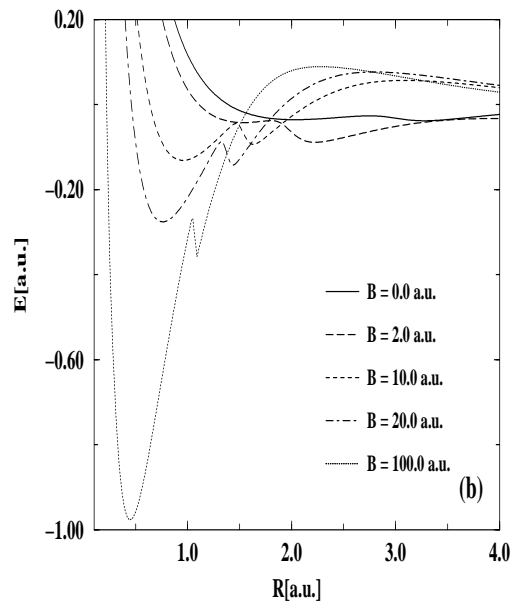
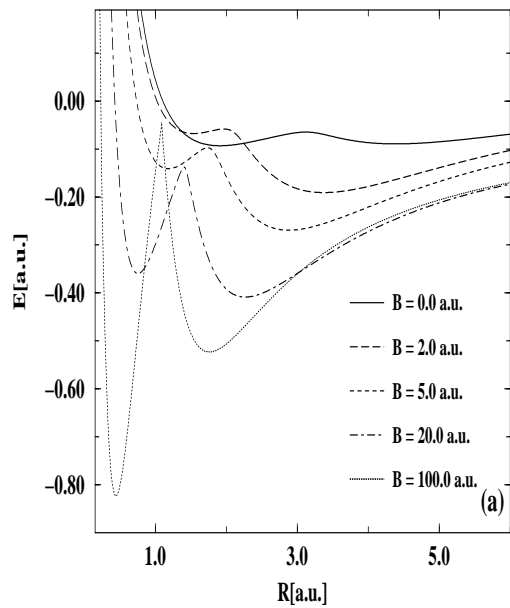
B	$R_{eq1}$	$E_{d1}$	$E_{t1}$	$R_{eq2}$	$E_{d2}$	$E_{t2}$	$R_{max}$	$E_{max}$	$\lim_{R \rightarrow \infty} E_{tot}$
0.0	2.03	0.081441	-0.636996	11.12	0.049964	-0.605519	5.65	-0.567698	-0.555555
0.001	2.03	0.081426	-0.636973	11.12	0.049971	-0.605518	5.64	-0.567692	-0.555547
0.005	2.03	0.081009	-0.636427	11.12	0.050053	-0.605471	5.64	-0.567528	-0.555418
0.01	2.03	0.080107	-0.635125	11.18	0.050291	-0.605309	5.67	-0.567116	-0.555018
0.05	2.04	0.074463	-0.619321	11.32	0.055802	-0.600660	5.45	-0.555308	-0.544858
0.1	2.05	0.071675	-0.594135	12.01	0.064313	-0.586773	5.40	-0.530941	-0.522460
0.2	2.03	0.062081	-0.540641	15.62	0.059632	-0.538198	5.42	-0.477396	-0.478566
0.5	1.94	0.035148	-0.363027	50.06	0.020138	-0.348017	5.20	-0.297160	-0.327879
1.0	1.78	0.033120	-0.024754				4.92	0.058491	0.008366
2.0	1.54	0.068597	0.735247				4.56	0.858143	0.803844
5.0	1.20	0.158473	3.267384				4.06	3.490593	3.425857
10.0	0.96	0.272912	7.770342				3.70	8.118636	8.043254
20.0	0.77	0.442635	17.118131				3.38	17.648590	17.560766
50.0	0.56	0.782055	45.957401				3.02	46.845692	46.739456
100.0	0.45	2.154264	94.799755				2.81	96.074966	96.954019

TABLE VI. Data for the third excited  $^1\Sigma_u$  state: Total energies  $E_{t1} - E_{t3}$  and dissociation energies  $E_{d1} - E_{d3}$  at the corresponding equilibrium internuclear distance, the equilibrium internuclear distances  $R_{eq1} - R_{eq3}$  and the total energy in the dissociation limit  $\lim_{R \rightarrow \infty} E_t$  as a function of the field strength  $0 \leq B \leq 100$  (all quantities are given in atomic units).

B	$R_{eq1}$	$E_{d1}$	$E_{t1}$	$R_{eq2}$	$E_{d2}$	$E_{t2}$	$R_{eq3}$	$E_{d3}$	$E_{t3}$	$\lim_{R \rightarrow \infty} E_{tot}$
0.0	2.00	0.078543	-0.634098	5.67	0.010196	-0.565751				-0.555555
0.001	2.00	0.078531	-0.634077	5.67	0.010194	-0.565740				-0.555546
0.005	2.00	0.078211	-0.633537	5.67	0.010161	-0.565487	33.89	0.000058	-0.555384	-0.555326
0.01	2.00	0.077103	-0.631765	5.67	0.010059	-0.564721	34.18	0.000338	-0.555000	-0.554662
0.05	2.01	0.063148	-0.603904	5.56	0.009249	-0.550005	42.09	0.004106	-0.544862	-0.540756
0.1	2.02	0.060038	-0.577452	5.50	0.009923	-0.527337	36.87	0.005048	-0.522462	-0.517414
0.2	2.00	0.057601	-0.522906	5.79	0.002238	-0.467543	33.92	0.000006	-0.465309	-0.465305
0.5	1.92	0.062864	-0.343463				34.57	0.000001	-0.280600	-0.280599
1.0	1.76	0.082384	-0.003776							0.078608
2.0	1.53	0.123535	0.757397							0.880932
5.0	1.19	0.224179	3.290662							3.514841
10.0	0.96	0.348221	7.794138							8.142359
20.0	0.76	0.528386	17.142170	3.52		17.707128				17.670556
50.0	0.56	0.882660	45.981219	3.09		46.897984				46.863879
100.0	0.45	1.266401	94.823274	2.82		96.127449				96.089675

# Figure 1





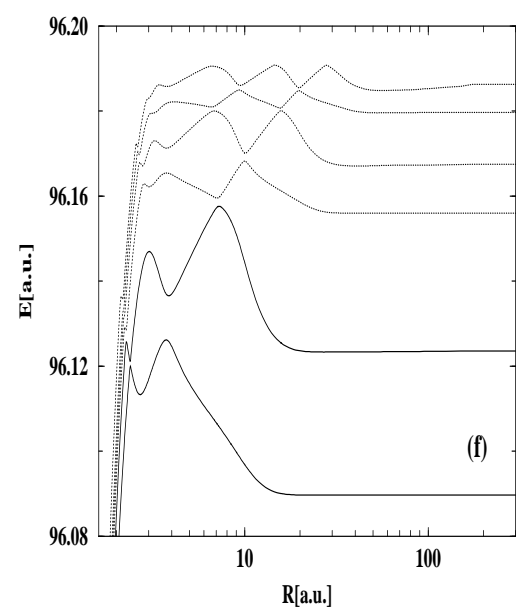
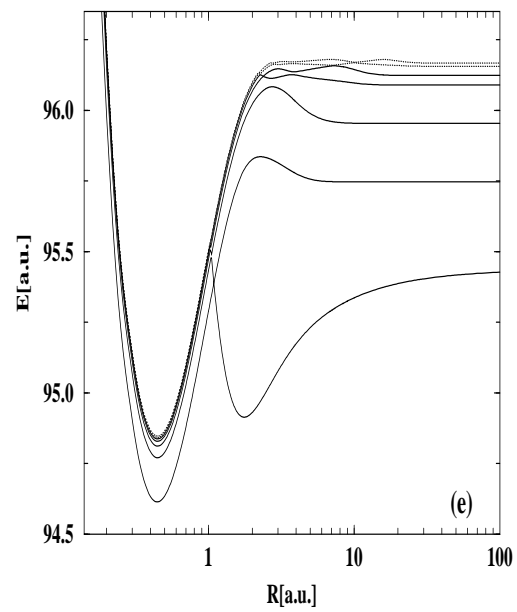
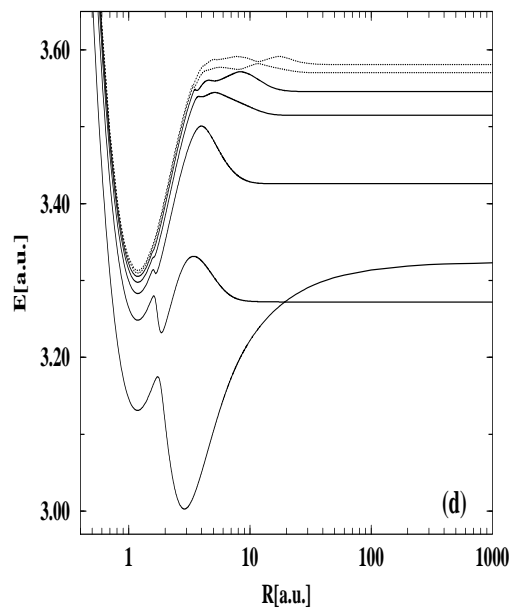
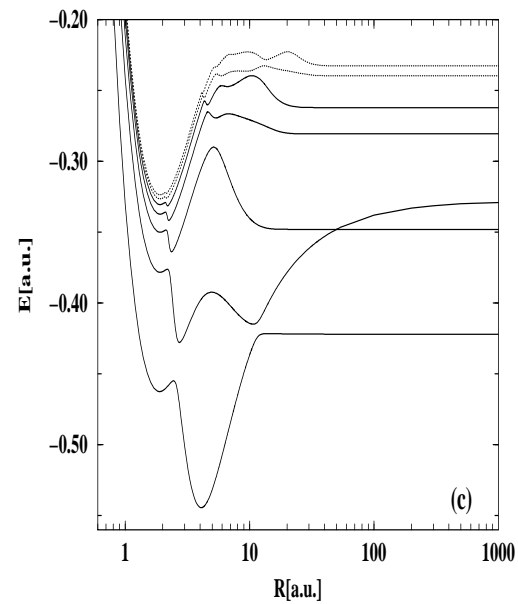
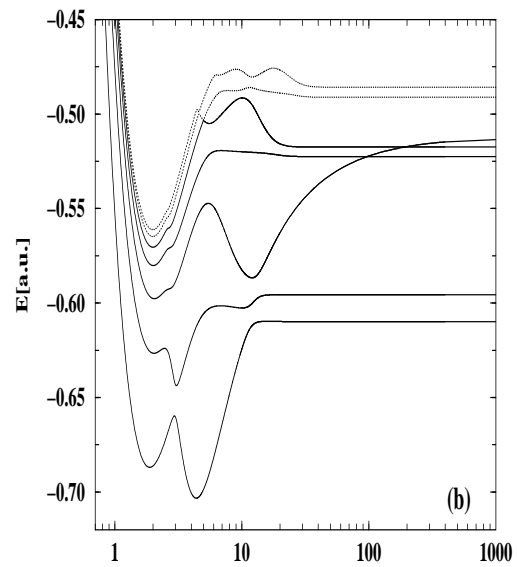
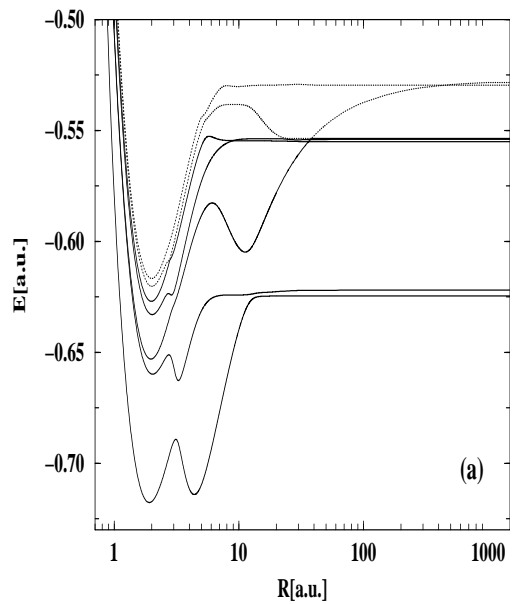


# Figure 4

